Journal of Biomechanics 46 (2013) 670–676

Contents lists available at SciVerse ScienceDirect

Journal of Biomechanics

journal homepage: www.elsevier.com/locate/jbiomech
www.JBiomech.com

Sensitivity, reliability and accuracy of the instant center of rotation calculation in the cervical spine during in vivo dynamic flexion-extension

Emma Baillargeon [a], William J. Anderst [b,*]

[a] University of Pittsburgh, Department of Bioengineering, USA
[b] University of Pittsburgh, Department of Orthopaedic Surgery, 3820 South Water Street, Pittsburgh, PA 15203, USA

ARTICLE INFO

Article history:
Accepted 24 November 2012

Keywords:
Helical axis
Center of rotation
Kinematics
Cervical disc replacement

ABSTRACT

The instant center of rotation (ICR) has been proposed as an alternative to range of motion (ROM) for evaluating the quality, rather than the quantity, of cervical spine movement. The purpose of the present study was to assess the sensitivity, reliability and accuracy of cervical spine ICR path calculations obtained during dynamic in vivo movement. The reliability and sensitivity of in vivo cervical spine ICR calculations were assessed by evaluating the effects of movement direction (flexion versus extension), rotation step size, filter frequency, and motion tracking error. The accuracy of the ICR path calculations was assessed through a simulation experiment that replicated in vivo movement of cervical vertebrae. The in vivo assessment included 20 asymptomatic subjects who performed continuous head flexion-extension movements while biplane radiographs were collected at 30 frames per second. In vivo motion of C2 through C7 cervical vertebrae was tracked with sub-millimeter accuracy using a volumetric model-based tracking technique. The finite helical axis method was used to determine ICRs between each pair of adjacent vertebra. The in vivo results indicate ICR path is not different during the flexion movement and the extension movement. In vivo, the path of the ICR can reliably be characterized within 0.5 mm in the SI and 1.0 mm in the AP direction. The inter-subject variability in ICR location averaged ± 1.2 mm in the SI direction and ± 2.2 mm in the AP direction. The computational experiment estimated the in vivo accuracy in ICR location was between 1.1 mm and 3.1 mm.

1. Introduction

Lateral radiographs collected at full-flexion and full-extension have traditionally been used to assess cervical spine kinematics, quantify normal motion, and diagnose abnormalities. These static radiographs are most often used to evaluate intervertebral range of motion (ROM) between adjacent cervical vertebrae. However, ROM has limited clinical application due to measurement inaccuracy inherent to the manual digitizing of vertebral landmarks and the wide inter subject variability in "normal" ROM reported for asymptomatic subjects (Dvorak et al., 1991; Frobin et al., 2002; Lind et al., 1989; Wu et al., 2007).

As an alternative to ROM, the instant center of rotation (ICR) has been proposed for evaluating the quality of movement and exploring abnormalities in the cervical spine (Bogduk and Mercer, 2000). Full-flexion and full-extension radiographs have previously been manually digitized to determine the ICR in asymptomatic subjects (Amevo et al., 1992,1991; Barrey et al., 2012; Dvorak et al., 1991) and symptomatic or surgical patients (Barrey et al., 2012; Amevo et al., 1992). While abnormalities in the ICR may correspond to specific pathologies (Bogduk et al., 1995), the clinical utility of measurements obtained from images collected only at the ends of the ROM remains limited. The dynamic function of muscles and ligaments cannot be assessed from static end ROM measurements, and end ROM data points are not necessarily representative of mid-range motion where the majority of our activities of daily living occur (Bible et al., 2010; Cobian et al., 2009). In addition, the ICR will change location during dynamic motion and may not be fully described by a single point (An and Chao, 1984).

In an attempt to fully characterize joint motion, the path of the ICR through a full range of motion, i.e. the centrode (Soudan et al., 1979), may be calculated. The centrode has been determined for various joints including the wrist (King et al., 1986), knee (Blankevoort et al., 1990; Sheehan, 2007; Van Den Bogert et al., 2008), lumbar spine (Ogston et al., 1986), and foot/ankle (Sawers and Hahn 2011; Sheehan 2010). Centrode information may be particularly valuable to clinicians, as the centrode indicates *how*

* Corresponding author. Tel.: +1 412 586 3946; fax: +1 412 586 3979.
E-mail address: anderst@pitt.edu (W.J. Anderst).

0021-9290/$ - see front matter © 2012 Elsevier Ltd. All rights reserved.
http://dx.doi.org/10.1016/j.jbiomech.2012.11.055

motion occurs between adjacent bones during continuous motion (i.e. motion quality), not simply *how much* motion occurs between adjacent bones (i.e. ROM). Furthermore, characterizing the centrode during cervical spine motion is currently of particular interest due to the recent FDA approval of several cervical disc replacement devices in the United States (Coric et al., 2011; Murrey et al., 2009; Sasso et al., 2011). These disc replacements have either fixed or variable centers of rotation, and it is not clear how well these designs mimic in vivo cervical spine function.

ICR calculations are notoriously sensitive to factors such as tracking error, marker placement, and rotation step size. Therefore, it is important that the experimental methods are thoroughly validated and expected errors are quantified prior to implementing these calculations in a new application (Crisco et al., 1994). Although parametric sensitivity analyses using simulated data may be used to identify factors influential to determining the ICR (Crisco et al., 1994; Halvorsen et al., 1999; Metzger et al., 2010; Panjabi et al., 1982), assessing the accuracy of ICR calculations obtained from in vivo data proves to be more difficult. In vivo, during dynamic motion, a "known" center of rotation is not available to use as a gold standard for comparison in parametric evaluations. In this situation, the accuracy of ICR calculations may be assessed through a simulation experiment designed to characterize the computational accuracy given the expected in vivo tracking error and marker distribution. Furthermore, the in vivo reliability may be assessed by analyzing multiple trials from the same subject, while the in vivo sensitivity may be assessed by a parametric evaluation of factors affecting the ICR calculation.

The purpose of the present study was to assess the sensitivity, reliability and accuracy of in vivo dynamic cervical spine ICR path calculations obtained using biplane radiographs and a volumetric model-based tracking algorithm. The in vivo sensitivity and reliability were evaluated with respect to movement direction (flexion versus extension), rotation step-size, filter frequency, and tracking error using a large cohort of asymptomatic subjects. The experimental accuracy was determined by a simulation experiment using parameters appropriate for the in vivo protocol (i.e. tracking noise, distance from bone to ICR, filter frequency, rotation step size).

2. Methods

2.1. In vivo data

Following Institutional Review Board (IRB) approval, data was collected from 20 asymptomatic subjects (13 F, 7 M; average age: 45.6 ± 5.7 yrs.) who provided informed consent to participate in this research study. Subjects were seated within a biplane X-ray system and, for each trial, directed to continuously move their head and neck through their entire range of flexion-extension. A metronome set at 40–44 beats per minute was used to ensure the participants moved at a continuous, steady pace to complete each full movement cycle in approximately 3 s. Radiographs were collected at 30 frames per second for 3 s for each trial of flexion-extension (X-ray parameters: 70 KV, 160 mA, 2.5 ms X-ray pulses, source-to-subject distance 140 cm). Radiographs were recorded for 2 or 3 separate trials for each subject (allowing for a rest period between trials), resulting in a total of 50 trials included in the present in vivo analysis. In addition, high-resolution CT scans ($0.29 \times 0.29 \times 1.25$ mm voxels) of the cervical spine (C2–C7) were acquired from each participant (GE Lightspeed 16). The effective radiation dose for each dynamic flexion-extension motion trial was estimated to be 0.16 mSv (determined using PCXMC simulation software, STUK, Helsinki, Finland). The effective dose of a cervical spine CT scan has been reported to be between 3.0 mSv and 4.36 mSv (Biswas et al., 2009; Fazel et al., 2009).

Bone tissue was segmented from the CT volume using a combination of commercial software (Mimics software, Materialise, Leuven, Belgium) and manual segmentation (Thorhauer et al., 2010). A three-dimensional (3D) model of each vertebra was generated from the segmented bone tissue. Markers were interactively placed on the 3D bone models to define bone-specific anatomic coordinate systems. In vivo bone motion of C2 through C7 vertebrae was tracked using a volumetric model-based tracking technique previously described in detail (Fig. 1) (Anderst et al., 2009,2011; Bey et al., 2006). This model-based tracking technique has been previously validated in vivo to have a precision of 0.33 mm or better for intervertebral translations and 1.1° for intervertebral rotations of the cervical spine (Anderst et al., 2011). Cervical spine intervertebral kinematics were determined following established standards for reporting spine kinematics (Kane et al., 1983; Wu et al., 2002). Intervertebral flexion-extension angle during dynamic movement trials was normalized to a trial collected with the participant in the static neutral position.

A series of ICR locations was calculated between each pair of adjacent vertebrae over the subject's full range of motion using the finite helical axis (FHA) method (Spoor and Veldpaus, 1980). Each ICR was defined as the intersection point of the computed FHA and the sagittal anatomical plane of the inferior vertebra. The anterior–posterior (AP) and superior–inferior (SI) location of each ICR was defined with respect to the inferior bone anatomic coordinate system and expressed as a percentage of the inferior bone size. The path of ICR positions during flexion-extension was interpolated at 1° increments of intervertebral flexion-extension to allow for comparison among trials, movement direction, and participants. ICR locations calculated to be more than 200% of inferior bone width or height (for AP ICR and SI ICR, respectively) from the inferior bone origin

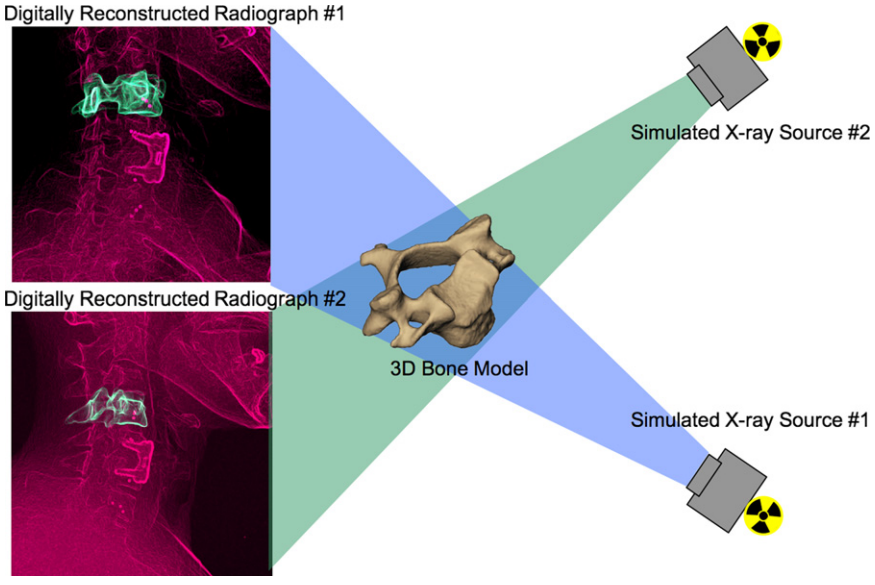

Fig. 1. An illustration of the virtual X-ray system for model-based tracking. A three-dimensional CT reconstruction of the bone was placed in a computer generated reproduction of the X-ray system. Simulated X-rays were then passed through the three-dimensional CT reconstruction to generate digitally reconstructed radiographs. Bone position and orientation were determined by optimizing the correlation between the digitally reconstructed radiographs (green in figure) and the edge-enhanced radiographs (red in figure). Figure adapted from Anderst et al., 2011. (For interpretation of the references to color in this figure legend, the reader is referred to the web version of this article.)

were excluded from analysis. Due to inter-subject variability in flexion and extension range of motion at each motion segment, and the fact that the ROM was not centered about the neutral position for all subjects, ICR data were available at different ranges of intervertebral flexion-extension for each participant (Fig. 2). Therefore, analysis was restricted to ICR values at 1° intervals that contained data from at least 6 participants (Fig. 2 and Table 1) as has been previously done for evaluating ICR repeatability (Sheehan, 2007).

The effects of movement direction (flexion versus extension), intervertebral rotation step-size (0.5°, 1.0°, and 2.0°), filter frequency (1.0 Hz, 2.0 Hz, 4.0 Hz) and in vivo tracking errors ($\pm 0.5°$, $\pm 1.0°$ rotation; ± 0.25 mm, ± 0.5 mm translation) on ICR location were evaluated. These filter frequencies were selected because a previous analysis of this in vivo kinematic data (Anderst et al., in press) indicated an optimal cutoff frequency of 1.7 Hz using residual analysis (Winter, 2009). A low-pass, 4th-order Butterworth filter was used to smooth the 6 DOF motion path of each bone (3 translations and 3 rotations). Differences in ICR location during the flexion and extension movements were calculated at each 1° increment of intervertebral flexion-extension for each motion segment. The average of these differences was then calculated across all intervertebral flexion-extension angles for each subject for analysis purposes (Fig. 3).

Within-subject trial-to-trial variability (i.e. reliability) in ICR locations was determined in a similar fashion by calculating differences among trials in ICR location at each corresponding 1° increment of intervertebral flexion-extension (after averaging corresponding flexion and extension ICRs for each trial) and then averaging across all intervertebral flexion-extension angles for each subject (Fig. 4).

Inter and intra-subject sensitivity to filter frequency and step size were determined by processing each trial for each individual at each level of filter frequency and step size (50 trials by 3 filter frequencies by 3 step sizes). The sensitivity to in vivo tracking error was assessed by systematically modifying the tracking results in each of the six degrees of freedom for one motion segment of one subject. Rotation tracking errors of $\pm 0.5°$ and $\pm 1.0°$ were introduced independently in each rotational degree of freedom, and tracking errors of ± 0.25 mm and ± 0.5 mm were introduced independently in each translational degree of freedom.

2.2. Simulated data

Simulated bone motion data was created to assess the effects of tracking error, distance from the moving bone to the ICR, filter frequency, and rotation step size on ICR accuracy. Values included in the parametric evaluation were selected to span the range of potential values encountered during in vivo cervical spine motion using the previously described in vivo testing conditions and equipment. An initial dataset of "perfect" 3D bone motion was generated to simulate intervertebral flexion-extension about a fixed center of rotation. The "moving bone" rotated through 15° of flexion-extension (from 8° extension to 7° flexion back to 8° extension) over 3.0 s, with data sampled at 30 Hz to replicate in vivo ROM and testing conditions. The "perfect" simulated bone motion followed a circular path about the ICR, with angular velocity varying in a sinusoidal pattern (highest at the center of motion, lowest at the ends) to replicate in vivo flexion-extension angular velocity. At its peak, the moving bone was rotating about the fixed bone at 40° per second, also representative of our in vivo recorded motion. The effect of tracking error was assessed by adding random, uniformly distributed 3D noise to the ideal dataset. Random 3D noise in the translation of the center of the moving bone (mean=0) was introduced at two levels: standard deviation=0.2 mm and standard deviation=0.3 mm. Random rotation noise about each axis of the moving bone (mean=0) was introduced at one level: standard deviation=1.0°. These noise values were representative of the previously reported in vivo tracking precision using the model-based tracking technique for the cervical spine (Anderst et al., 2011). It should be noted that the noise was added to the bone model motion, thus all "points" on the bone remained in the same location relative to each other after the noise was added. This replicated our model-based tracking technique. A low-pass, 4th-order Butterworth filter was used to smooth the 3D bone motion using filter frequencies of 1.0 Hz, 2.0 Hz and 4.0 Hz as part of the parametric evaluation. Three distances from the known center of rotation to the center of the bone model were evaluated: 14 mm, 18 mm and 22 mm. These ICR-to-bone center distances were selected to span the potential range of distances between the geometric center of each cervical vertebra and its center of rotation. Rotation step sizes of 1.0° and 2.0° were selected for evaluation of the simulated data. As in the in vivo experiment, the ICR paths were interpolated at 1° increments of rotation and flexion ICR values were averaged with extension ICR values at corresponding flexion-extension angles, yielding 16 ICR values for each flexion-extension cycle. The average error in these ICR values was determined by the distance from the known ICR on the sagittal plane of the "fixed" bone (a point at 0,0) to the calculated ICR: Average Error = $\sum \sqrt{(X_{calculated})^2+(Y_{calculated})^2}/n$ where n is the number of ICR values calculated. The simulation was repeated 20 times for each combination of parameters investigated (noise, filter frequency, step size, and distance between bone and ICR), resulting in 320 ICRs for each combination of parameters (16 ICRs X 20 repeated simulations).

3. Results

3.1. In vivo data

The total number of ICR locations included in the analysis varied by vertebral level and rotation step size (Table 2). The number of outliers excluded from analysis was greatest at

Table 1
Intervertebral flexion-extension range of motion included in the analysis. Negative angles indicate extension ROM, positive values indicate flexion ROM.

Motion segment	Step size (°)		
	0.5	1.0	2.0
C2/C3	−4 to +6	−3 to +5	−3 to +5
C3/C4	−7 to +7	−7 to +7	−5 to +6
C4/C5	−9 to +8	−9 to +7	−8 to +7
C5/C6	−6 to +8	−6 to +7	−5 to +6
C6/C7	−5 to +8	−4 to +7	−4 to +7

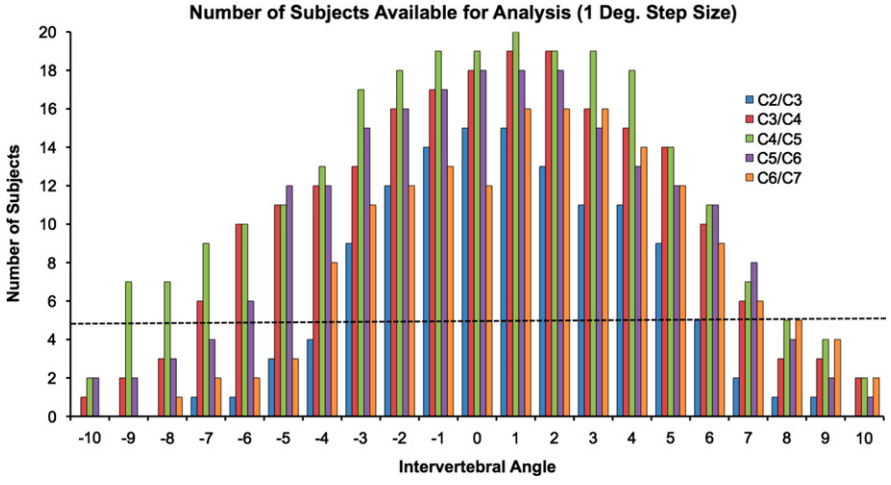

Fig. 2. Chart showing the number of subjects with available data at each intervertebral flexion-extension angle for each cervical motion segment. Horizontal axis indicates intervertebral flexion (positive values) and extension (negative values) relative to the static neutral orientation. Intervertebral flexion-extension angles were included in the analysis when data from at least 6 subjects was available. The dashed line indicates the separation between sufficient and too few subjects. This chart shows data only for the 1° step size. The distribution of available data was similar for 0.5° and 2° step sizes (Table 1). Differences in ROM and missing data for a portion of the flexion or extension motion account for differences in the number of subjects providing data at each flexion-extension angle.

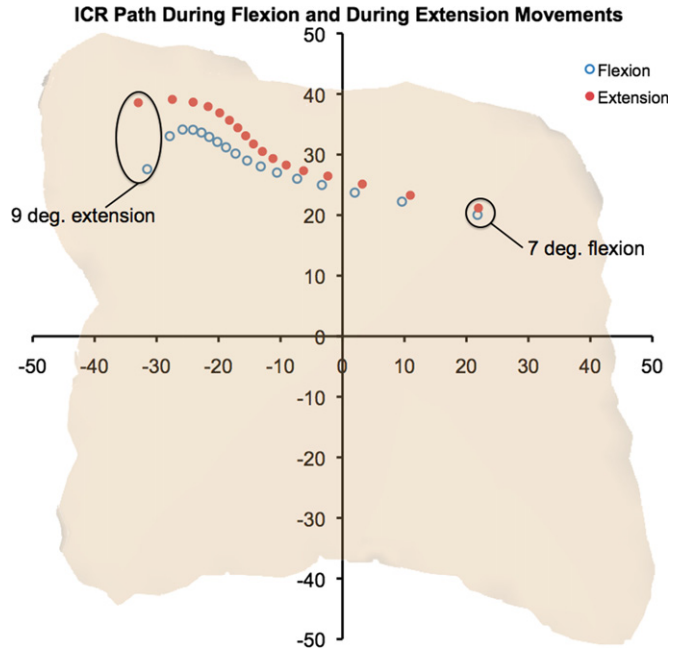

Fig. 3. Flexion versus extension ICR comparison from a representative trial. The continuous path of the ICR of the superior vertebra relative to the inferior vertebra was interpolated at 1° increments during the flexion (blue, open circles) and extension (red, filled circles) movement directions and expressed in the anatomic coordinate system of the inferior vertebral body. ICR locations during flexion and extension were compared at corresponding angles of intervertebral rotation (e.g. 5° flexion vs. 5° extension). Units on the horizontal and vertical axes are percent bone size (x=% bone depth, y=% bone height). A cross-sectional view of the inferior vertebral body is provided in the background to provide anatomic context. (For interpretation of the references to color in this figure legend, the reader is referred to the web version of this article.)

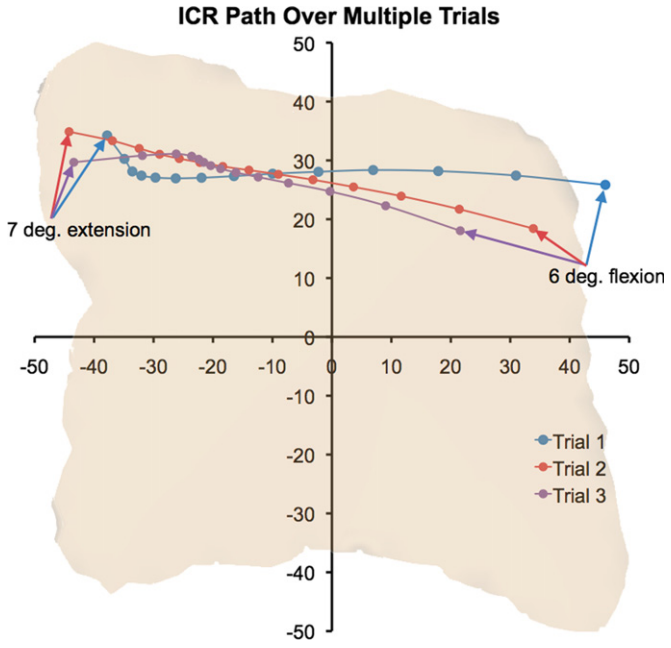

Fig. 4. The path of the ICR over three flexion-extension trials for one subject. Trial-to-trial variability was determined by calculating ICR location differences at corresponding angles of intervertebral rotation over all trials for a given subject. Three trials from a representative subject are shown with data points at each 1° increment of intervertebral rotation from 7° extension to 6° flexion.

the C2/C3 motion segment (1.6% of the total ICRs calculated after interpolation at C2/C3) and 0.5° step size (0.6% of the total ICRs calculated after interpolation using 0.5° step size).

Average bone height and bone depth were 13.5 mm and 14.7 mm, respectively. Inter-subject variability (defined as the 95% confidence interval (CI)) in bone height and depth was ±0.7 mm and ±1.1 mm, respectively. ICR results were calculated as a percentage of bone size for each individual. Therefore, on average, a one percent increment in bone height represented 0.135 mm and a one percent increment in bone depth represented 0.147 mm (Table 3).

Average differences between flexion and extension motion ICR locations were always less than 5% of bone size and the 95% confidence intervals included zero for each vertebral level, each rotation step size, and each filter frequency (Fig. 5). This indicates ICR locations calculated during the flexion motion were not different from those calculated at corresponding intervertebral angle during the extension motion. The 2 Hz filter frequency and 2° step size produced the minimum combination of intra-subject differences (the size of the bars in Fig. 5) and inter-subject variability (the size of the 95% CIs in Fig. 5) in flexion versus extension differences.

Trial-to-trial variability increased at the 4 Hz filter frequency and consistently decreased with increasing step size (Fig. 6). Within-subject trial-to-trial variability in the SI direction was minimized by using the 1 Hz filter and 2° step size (3.7% bone height, which corresponds to 0.5 mm), while variability in the AP direction was minimized by using the 2 Hz filter frequency and a 2° step size (6.7% bone depth, which corresponds to 1.0 mm). Inter-subject differences in trial-to-trial variability, represented by the size of the 95% CI bars in Fig. 6, consistently decreased with increasing step size.

Table 2
The number of ICR locations included in the in vivo analysis at each vertebral level and flexion-extension rotation step size after interpolating all ICR data to 1 degree intervals. Values in parentheses indicate the number of ICR outliers rejected for analysis.

Motion segment	Step size (°)			Total
	0.5	1.0	2.0	
C2/C3	564 (13)	512 (8)	425 (3)	1501 (24)
C3/C4	927 (4)	889 (2)	781 (0)	2597 (6)
C4/C5	1077 (1)	1031 (0)	926 (1)	3034 (2)
C5/C6	931 (0)	873 (0)	763 (0)	2567 (0)
C6/C7	753 (7)	687 (3)	581 (3)	2021 (13)
Total	4252 (25)	3992 (13)	3476 (7)	

The inter-subject variability in ICR location, characterized by the 95% CI of the mean ICR location at each intervertebral flexion-extension angle, averaged ±1.2 mm in the SI direction and ±2.2 mm in the AP direction across all intervertebral flexion-extension angles and all motion segments.

ICR location was most sensitive to translation tracking errors within the flexion-extension plane (Table 4). Small errors in AP and SI tracking (±0.25 mm) led to substantial alterations in ICR location (86% and 80% bone size), while small errors in FE tracking (±0.5°) led to smaller, yet substantial changes in ICR location (46% bone size).

3.2. Simulated data

Filtering the simulated data at 1 Hz, 2 Hz and 4 Hz resulted in average ICR location errors of 1.1 mm, 3.1 mm and 6.8 mm, respectively, after applying noise levels appropriate for the given tracking system (Fig. 7). The evaluated step size and noise parameters had little effect on ICR error at lower cutoff frequencies of 1 Hz and 2 Hz. The average ICR errors in the 18 mm and 22 mm bone-to-ICR configurations were different from 14 mm

Table 3
Average values and 95% confidence intervals (CI) for bone height and depth. All units are mm.

	Bone height			Bone depth		
	Lower 95% CI	Mean	Upper 95% CI	Lower 95% CI	Mean	Upper 95% CI
C3	13.1	13.8	14.5	13.0	13.7	14.5
C4	12.7	13.3	13.8	13.4	14.3	15.2
C5	12.4	12.9	13.4	14.0	15.1	16.3
C6	12.6	13.0	13.4	14.4	15.5	16.7
C7	14.0	14.5	15.0	13.8	14.8	15.8

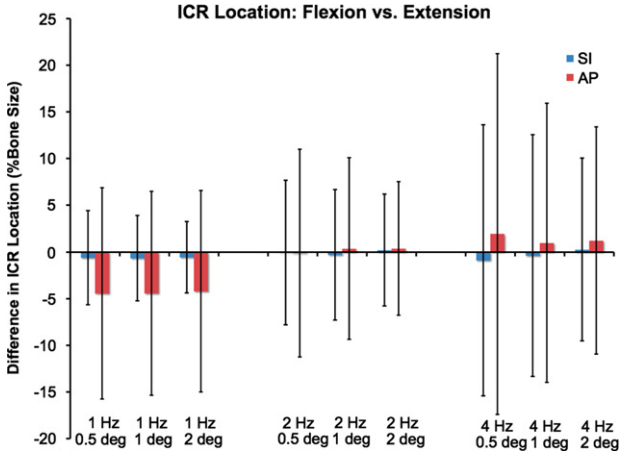

Fig. 5. Average differences in ICR location during the flexion movement and the extension movement at corresponding angles of intervertebral rotation. Solid bars represent within-subject average location differences in the superior–inferior (blue bars) and anterior–posterior (red bars) directions. Error bars represent the 95% confidence interval of the inter-subject variability in flexion versus extension ICR location. These means and confidence intervals were obtained by averaging data from all motion segments (C2/C3 through C6/C7) of all subjects. (For interpretation of the references to color in this figure legend, the reader is referred to the web version of this article.)

bone-to-ICR errors by only 0.1 mm and 0.02 mm, respectively, across all combinations of filter frequency and step size.

4. Discussion

The in vivo results indicate that ICR locations are not different between the flexion movement and the extension movement at corresponding intervertebral flexion-extension angles. This finding was consistent across all filter frequencies and all step sizes. This suggests that differences in loading during the flexion motion versus the extension motion do not appreciably affect the motion path between adjacent vertebrae, at least in this group of asymptomatic subjects. The small average difference between flexion and extension ICR for the 2 Hz filter and 2° step size, in combination with the narrow 95% CI of the difference in flexion versus extension ICR path ($\pm$0.8 mm in the SI direction and $\pm$1.0 mm in the AP direction), suggests the ICR path may be a sensitive indication of dysfunction during the flexion-extension movement. This information may be used to evaluate a clinical cohort, such as whiplash patients, who have soft tissue injury that may preferentially affect movement in flexion or extension. It is typically difficult to identify tissue damage in whiplash patients (Curatolo et al., 2011), and differences between flexion and extension ICR paths may address this clinical challenge. The consistent ICR path during flexion and during extension implies that for a motion-preserving disc replacement to replicate in vivo motion, the disc replacement should allow a single path of the ICR for flexion and extension movements (i.e. there is no "hysteresis" in the flexion-extension ICR path).

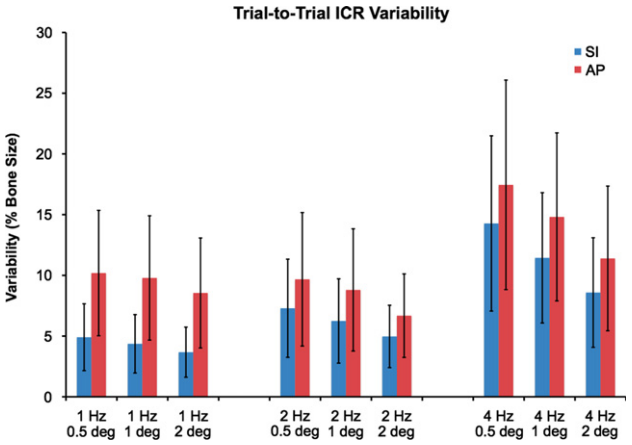

Fig. 6. Trial-to-trial variability in the ICR at corresponding angles of intervertebral flexion-extension as a function of filter frequency and step size. Solid bars indicate within-subject variability, while error bars indicate 95% confidence intervals of inter-subject variability. These means and confidence intervals were obtained by averaging data from all motion segments (C2/C3 through C6/C7) of all subjects.

Table 4
Sensitivity of ICR to model-based tracking errors. Translation tracking errors were introduced independently in the anterior–posterior (AP), medial-lateral (ML) and superior–inferior (SI) directions, as well as rotation tracking errors about the lateral bend (LB), twist (TW) and flexion-extension (FE) axes. Values indicate change in ICR location expressed as a % of bone size.

	Sensitivity to translation tracking errors		
	Tracking error	+/−0.25 mm (%)	+/−0.50 mm (%)
Translation direction	AP	86	172
	ML	8	15
	SI	80	159
	Sensitivity to rotation tracking errors		
	Tracking error	+/−0.5°(%)	+/−1.0°(%)
Rotation direction	LB	4	11
	TW	16	44
	FE	46	85

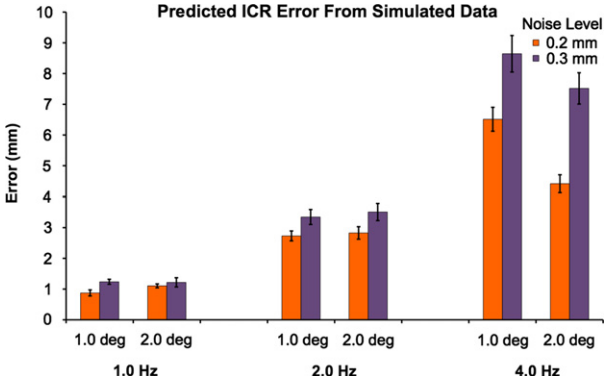

Fig. 7. Average ICR error using simulated data with 3D noise added. The effects of filter frequency (1.0 Hz, 2.0 Hz and 4.0 Hz) and rotation step size (1.0° and 2.0°) are shown as a function of 3D translation noise (0.2 mm and 0.3 mm). Rotation noise was set to 1° about each of the three axes. Data is shown for a 14 mm distance between fixed ICR and marker locations. Error bars represent 95% confidence interval of the ICR error.

In vivo, the path of the ICR can reliably be characterized within 0.5 mm in the SI and 1.0 mm in the AP direction, on average. This trial-to-trial variability in the ICR path, at least when restricted to mid-range motion of healthy controls, is comparable to the trial-to-trial variability in total ROM (0.1 mm in translation and 0.4° in rotation) (Anderst et al., in press). Given these trial-to-trial variability results, it appears that collecting 2 to 3 trials of flexion-extension movement is sufficient to reliably estimate the path of the center of rotation in vivo with a precision of 1.0 mm or better. It should be noted that these trial-to-trial variability measures include variability due to tracking errors each trial and variability due to differences in movement by the subject from one trial to the next. We have previously demonstrated that inter-operator variability in running the automated software to track individual bone models is 0.02 mm in translation and 0.06° in rotation (Anderst et al., 2011).

Although analytical models have been developed to estimate ICR calculation error due to marker cluster design (i.e. the number of markers and their locations relative to the ICR) (Page et al., 2006), the current application is unique in that entire bone models are tracked, not individual points on the bone. Therefore, the errors in tracking marker locations (if there were markers placed on each bone) would not be independent. The computational experiment using "ideal" simulated data with added noise suggests that the expected in vivo accuracy in the ICR calculation is between 1.1 mm and 3.1 mm at filter frequencies of 1 Hz and 2 Hz, respectively. It should be noted that the noise values applied for the simulation study were obtained from a previous in vivo validation study that required placing fiducial markers closely together in the cervical vertebrae (Anderst et al., 2011). Close placement of fiducial markers may have limited the accuracy of the "gold standard" reference values used to evaluate the model-based tracking accuracy. For example, in practice, the trial-to-trial variability in intervertebral ROM (Anderst et al., in press) was approximately one half of the variability expected given the previously reported accuracy of the model-based tracking system. Therefore, it is possible the noise added in the simulated experiment was approximately 2 times higher than the tracking error achieved in practice.

The tracking errors estimated from simulated data are lower than several previous reports of ICR accuracy simulation experiments (Crisco et al., 1994; Panjabi, 1979) due to three factors: (1) the small distance between the bone and the ICR, (2) the tracking of the entire bone model rather than individual points on the bone, and (3) the filtering of tracked data. Collecting continuous data at a high sample rate, then filtering the tracked data, clearly reduces the error associated with calculating the ICR. Additionally, a previous study has concluded that the small-step-size sensitivity of the ICR no longer applies following low-pass smoothing of data acquired at a relatively high sample rate, and the ICR may be accurately calculated for even small rotations (Woltring et al., 1994).

The current study was designed to assess the sensitivity, reliability and accuracy of a model-based tracking system for determining the ICR at each cervical motion segment during in vivo flexion-extension. Potential clinical applications for this information include assessing the effects of surgery (e.g. arthrodesis, disc replacement) on the ICR path of motion segments adjacent to the surgery and identifying mechanical alterations following injury (e.g. whiplash). A limitation of the current study is that the ICR analysis was limited to the mid-range of motion common to many subjects and the ICR at the ends of the ROM were generally not included in the analysis. Additionally, this study only reported variability within a single test session; inter-session reliability in ICR calculations remains to be determined.

Conflict of interest statement

None of the authors have financial or personal relationships with other people or organizations that could inappropriately influence (bias) this work. The study sponsors had no influence on the study design, data collection or interpretation for this work.

Acknowledgment

This project was supported by Grant no. R03-AR056265 from NIH/NIAMS and by a 21st Century Development Grant from the Cervical Spine Research Society. This work was also supported by a NSF Graduate Research Fellowship. The authors thank Jonathan Foster for his assistance with writing Matlab code for this project.

References

Amevo, B., Aprill, C., Bogduk, N., 1992. Abnormal instantaneous axes of rotation in patients with neck pain. Spine 17 (7), 748–756.
Amevo, B., Worth, D., Bogduk, N., 1991. Instantaneous axes of rotation of the typical cervical motion segments: a study in normal volunteers. Clinical Biomechanics 6, 111–117.
An, K.N., Chao, E.Y., 1984. Kinematic analysis of human movement. Annals of Biomedical Engineering 12 (6), 585–597.
Anderst, W., Donaldson, W., Lee, J., Kang, J. Six degree of freedom cervical spine range of motion during dynamic flexion-extension in single-level anterior arthrodesis patients and asymptomatic controls. Journal of Bone and Joint Surgery, http://dx.doi.org/10.2106/JBJS.K.01733, in press.
Anderst, W., Zauel, R., Bishop, J., Demps, E., et al., 2009. Validation of three-dimensional model-based tibio-femoral tracking during running. Medical Engineering and Physics 31 (1), 10–16.
Anderst, W.J., Baillargeon, E., Donaldson 3rd, W.F., Lee, J.Y., et al., 2011. Validation of a noninvasive technique to precisely measure in vivo three-dimensional cervical spine movement. Spine 36 (6), E393–400.
Barrey, C., Champain, S., Campana, S., Ramadan, A., et al., 2012. Sagittal alignment and kinematics at instrumented and adjacent levels after total disc replacement in the cervical spine. European Spine Journal 21 (8), 1648–1659.
Bey, M.J., Zauel, R., Brock, S.K., Tashman, S., 2006. Validation of a new model-based tracking technique for measuring three-dimensional, in vivo glenohumeral joint kinematics. Journal of Biomechanical Engineering 128 (4), 604–609.
Bible, J.E., Biswas, D., Miller, C.P., Whang, P.G., et al., 2010. Normal functional range of motion of the cervical spine during 15 activities of daily living. Journal of Spinal Disorders and Techniques 23 (1), 15–21.
Biswas, D., Bible, J.E., Bohan, M., Simpson, A.K., et al., 2009. Radiation exposure from musculoskeletal computerized tomographic scans. Journal of Bone and Joint Surgery American volume 91 (8), 1882–1889.
Blankevoort, L., Huiskes, R., De Lange, A., 1990. Helical axes of passive knee joint motions. Journal of Biomechanics 23 (12), 1219–1229.
Bogduk, N., Amevo, B., Pearcy, M., 1995. A biological basis for instantaneous centres of rotation of the vertebral column. Proceedings of the Institution of Mechanical Engineers Part H-Journal of Engineering in Medicine 209 (3), 177–183.
Bogduk, N., Mercer, S., 2000. Biomechanics of the cervical spine. I: Normal kinematics. Clinical Biomechanics 15 (9), 633–648.
Cobian, D.G., Sterling, A.C., Anderson, P.A., Heiderscheit, B.C., 2009. Task-specific frequencies of neck motion measured in healthy young adults over a five-day period. Spine 34 (6), E202–207.
Coric, D., Nunley, P.D., Guyer, R.D., Musante, D., et al., 2011. Prospective, randomized, multicenter study of cervical arthroplasty: 269 patients from the Kineflex C artificial disc investigational device exemption study with a minimum 2-year follow-up: clinical article. Journal of Neurosurgery Spine 15 (4), 348–358.
Crisco 3rd, J.J., Chen, X., Panjabi, M.M., Wolfe, S.W., 1994. Optimal marker placement for calculating the instantaneous center of rotation. Journal of Biomechanics 27 (9), 1183–1187.
Curatolo, M., Bogduk, N., Ivancic, P.C., McLean, S.A., et al., 2011. The role of tissue damage in whiplash-associated disorders: discussion paper 1. Spine (Phila Pa 1976) 36 (25), S309–315.
Dvorak, J., Panjabi, M.M., Novotny, J.E., Antinnes, J.A., 1991. In vivo flexion/extension of the normal cervical spine. Journal of Orthopedic Research 9 (6), 828–834.
Fazel, R., Krumholz, H.M., Wang, Y., Ross, J.S., et al., 2009. Exposure to low-dose ionizing radiation from medical imaging procedures. New England Journal of Medicine 361 (9), 849–857.
Frobin, W., Leivseth, G., Biggemann, M., Brinckmann, P., 2002. Sagittal plane segmental motion of the cervical spine. A new precision measurement protocol and normal motion data of healthy adults. Clinical Biomechanics 17 (1), 21–31.

Halvorsen, K., Lesser, M., Lundberg, A., 1999. A new method for estimating the axis of rotation and the center of rotation. Journal of Biomechanics 32 (11), 1221–1227.

Kane, T., Likins, P., Leivseth, G., 1983. Spacecraft Dynamics. McGraw-Hill, New York.

King, G.J., McMurtry, R.Y., Rubenstein, J.D., Gertzbein, S.D., 1986. Kinematics of the distal radioulnar joint. Journal of Hand Surgery American Volume 11 (6), 798–804.

Lind, B., Sihlbom, H., Nordwall, A., Malchau, H., 1989. Normal range of motion of the cervical spine. Archives of Physical Medicine and Rehabilitation 70 (9), 692–695.

Metzger, M.F., Faruk Senan, N.A., O'Reilly, O.M., Lotz, J.C., 2010. Minimizing errors associated with calculating the location of the helical axis for spinal motions. Journal of Biomechanics 43 (14), 2822–2829.

Murrey, D., Janssen, M., Delamarter, R., Goldstein, J., et al., 2009. Results of the prospective, randomized, controlled multicenter Food and Drug Administration investigational device exemption study of the ProDisc-C total disc replacement versus anterior discectomy and fusion for the treatment of 1-level symptomatic cervical disc disease. Spine Journal 9 (4), 275–286.

Ogston, N.G., King, G.J., Gertzbein, S.D., Tile, M., et al., 1986. Centrode patterns in the lumbar spine. Baseline studies in normal subjects. Spine (Phila Pa 1976) 11 (6), 591–595.

Page, A., De Rosario, H., Mata, V., Hoyos, J.V., et al., 2006. Effect of marker cluster design on the accuracy of human movement analysis using stereophotogrammetry. Medical and Biological Engineering and Computing 44 (12), 1113–1119.

Panjabi, M.M., 1979. Centers and angles of rotation of body joints: a study of errors and optimization. Journal of Biomechanics 12 (12), 911–920.

Panjabi, M.M., Goel, V.K., Walter, S.D., Schick, S., 1982. Errors in the center and angle of rotation of a joint: an experimental study. Journal of Biomechanical Engineering 104 (3), 232–237.

Sasso, R.C., Anderson, P.A., Riew, K.D., Heller, J.G., 2011. Results of cervical arthroplasty compared with anterior discectomy and fusion: four-year clinical outcomes in a prospective, randomized controlled trial. Journal of Bone and Joint Surgery American volume 93 (18), 1684–1692.

Sawers, A., Hahn, M.E., 2011. Trajectory of the center of rotation in non-articulated energy storage and return prosthetic feet. Journal of Biomechanics 44 (9), 1673–1677.

Sheehan, F.T., 2007. The finite helical axis of the knee joint (a non-invasive in vivo study using fast-PC MRI). Journal of Biomechanics 40 (5), 1038–1047.

Sheehan, F.T., 2010. The instantaneous helical axis of the subtalar and talocrural joints: a non-invasive in vivo dynamic study. Journal of Foot and Ankle Research 3, 13.

Soudan, K., Van Audekercke, R., Martens, M., 1979. Methods, difficulties and inaccuracies in the study of human joint kinematics and pathokinematics by the instant axis concept. Example: the knee joint. Journal of Biomechanics 12 (1), 27–33.

Spoor, C.W., Veldpaus, F.E., 1980. Rigid body motion calculated from spatial co-ordinates of markers. Journal of Biomechanics 13 (4), 391–393.

Thorhauer, E., Miyawaki, M., Illingworth, K., Holmes, A., et al., 2010. Accuracy of Bone and Cartilage Models Obtained from CT and MRI. American Society of Biomechanics, Providence, RI.

van den Bogert, A.J., Reinschmidt, C., Lundberg, A., 2008. Helical axes of skeletal knee joint motion during running. Journal of Biomechanics 41 (8), 1632–1638.

Winter, D.A., 2009. Biomechanics and Motor Control of Human Movement, 4th Edition Wiley, Hoboken, New Jersey.

Woltring, H.J., Long, K., Osterbauer, P.J., Fuhr, A.W., 1994. Instantaneous helical axis estimation from 3-D video data in neck kinematics for whiplash diagnostics. Journal of Biomechanics 27 (12), 1415–1432.

Wu, G., Siegler, S., Allard, P., Kirtley, C., et al., 2002. ISB recommendation on definitions of joint coordinate system of various joints for the reporting of human joint motion-part I: ankle, hip, and spine. International society of biomechanics. Journal of Biomechanics 35 (4), 543–548.

Wu, S.K., Kuo, L.C., Lan, H.C., Tsai, S.W., et al., 2007. The quantitative measurements of the intervertebral angulation and translation during cervical flexion and extension. European Spine Journal 16 (9), 1435–1444.